Electrodiffusion Diagnostics of the Near-Wall Flows*

J. TIHON

Institute of Chemical Process Fundamentals,
Academy of Sciences of the Czech Republic, CZ-165 02 Prague
e-mail: tihon@icpf.cas.cz

Received 23 April 2001

The electrodiffusion method has been used to investigate the structure of near-wall turbulence. Two techniques recently used for fabrication of the multi-segment electrodiffusion probes are presented. The measurements performed in two experimental channel flows have demonstrated the application of such directionally sensitive probes under unsteady flow conditions. The traditional three-segment electrode provided valuable information on the recirculating flow structure behind a backward-facing step. The microelectrodes prepared by the new photolithography technique have been used to assess the influence of high polymer additives on spatial and temporal correlations of the flow fluctuations close to the wall.

Coherent structures in turbulent flow are recently a subject of considerable interest in turbulence research. The introduction and progress of new experimental techniques (LDA, PIV, visualizations, *etc.*) enables to identify the near-wall flow structures experimentally. The advanced computer technology has also contributed to the study of wall-bounded turbulence. Nevertheless, the near-wall region of the flow, which is experimentally difficult to investigate, has still received insufficient attention. This region, usually defined as that located between the wall and the inner boundary of the logarithmic part of the velocity profile, is an important one, because it is the place where viscosity strongly interacts with turbulence.

The electrodiffusion method, based on the measurement of the limiting diffusion current of the ferricyanide ions reduction at a small working electrode, can be used for the wall shear rate mapping. The principles of the method were explained exhaustively in the review by *Hanratty* and *Campbell* [1]. The fact, that the flush-mounted probes do not interfere with the flow, is the main advantage of this method. From the early sixties, when the method was first applied, the technique of probe fabrication was significantly improved [2—4] and some problems connected with the probes frequency response successfully solved [5—8]. The traditional technique of probe fabrication is based on gluing of platinum sensors directly into the wall. This technique was improved by *Sobolík et al.* [3] to produce the versatile multi-segment probes, which are sensitive to the near-wall flow direction. The new photolithography technique has been proposed by *Deslouis et al.* [4] to turn out the array of small microelectrodes, which can be very complicated and at the same time precisely patterned.

Both these techniques recently used for the probe fabrication are presented in this paper. The electrodiffusion measurements carried out in two different flow channels demonstrate the application of such directionally sensitive probes for diagnostics of the flow in the near-wall region.

THEORETICAL

The electrodiffusion method is based on the measurement of the limiting electric current passing through a small electrode, which is flush-mounted into the wall of an experimental channel. A voltage applied to the electrochemical cell, which consists of this working electrode and the larger counter electrode, drives a redox reaction at the electrode surfaces. Under conditions for which the rate of the involved electrochemical reaction is fast enough to consider that the concentration of the reacting ions is zero at the electrode, the measured current is fully controlled by convective diffusion only. If the length of this electrode is very small in the flow direction, the concentration boundary layer on the electrode is thin, thus the flow velocity varies linearly throughout the thickness of this boundary layer and the measured current is proportional to the wall shear rate. The local current density, i, measured on the electrode surface can be calculated according to the relationship

*Presented at the 28th International Conference of the Slovak Society of Chemical Engineering, Tatranské Matliare, 21—25 May 2001.

$$i = 0.538nFc_0D^{2/3}l^{-1/3}s^{1/3} \quad (1)$$

where n is the number of electrons involved in the redox reaction, F is the Faraday constant, c_0 is the bulk concentration of active ions, D is their diffusion coefficient, l is the local distance measured from the electrode front edge, and s is the wall-shear rate. The total probe current can be obtained by integration of eqn (*1*) over an entire surface of the working electrode. If flow fluctuations are slow enough, the quasi-steady relation can be applied to relate the wall shear rate s to the limiting diffusion current I

$$I = Ks^{1/3} \quad (2)$$

where K is the calibration constant dependent on a geometrical configuration of the electrode.

The multi-segment probes are suitable for the simultaneous measurement of instantaneous values of the wall shear rate and the flow direction close to the wall. The three-segment electrode, which has a circular shape divided into three identical segments, is a typical representative of this kind of probes. In this case, the total probe current is equal to the sum of the current contributions of individual segments I_s. This total current depends only on the absolute value of the wall shear rate and not on the probe configuration with respect to the flow direction. However, this probe configuration determines the individual I_s values. Consequently, the ratio I_s/I is only a function of the flow direction angle Φ and can be expressed as a sum of the terms

$$\frac{I_s}{I} = A_{s0} + \sum_{m=1}^{M} [A_{sm}\cos(m\Phi) + B_{sm}\sin(m\Phi)] \quad (3)$$

which are called the probe directional characteristics according to *Sobolík et al.* [3]. As real probes do not have geometrically identical segments, the coefficients A_{sm} and B_{sm} must be determined experimentally. An example of such directional calibration is presented in Fig. 1. The streamwise, s_x, and transverse, s_z, components of the wall shear rate can be calculated from the simple relationships: $s_x = s\cos\Phi$ and $s_z = s\sin\Phi$.

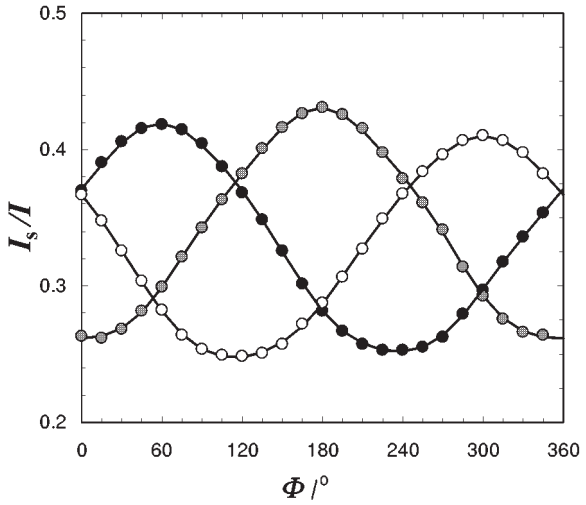

Fig. 1. Directional characteristics of the three-segment probe. Circles: calibration data for the segment 1 (black), 2 (grey), and 3 (white). Lines: fits of data for the segments by using eqn (*3*) with the parameter $m = 6$.

EXPERIMENTAL

The Backward-Facing Step Flow

A schematic diagram of the backward-facing step apparatus including the flow situation inside the channel is shown in Fig. 2. The rectangular experimental channel (70 mm in height, 0.22 m in width, and 1.6 m in length) was made of plexiglass. A plexiglass block,

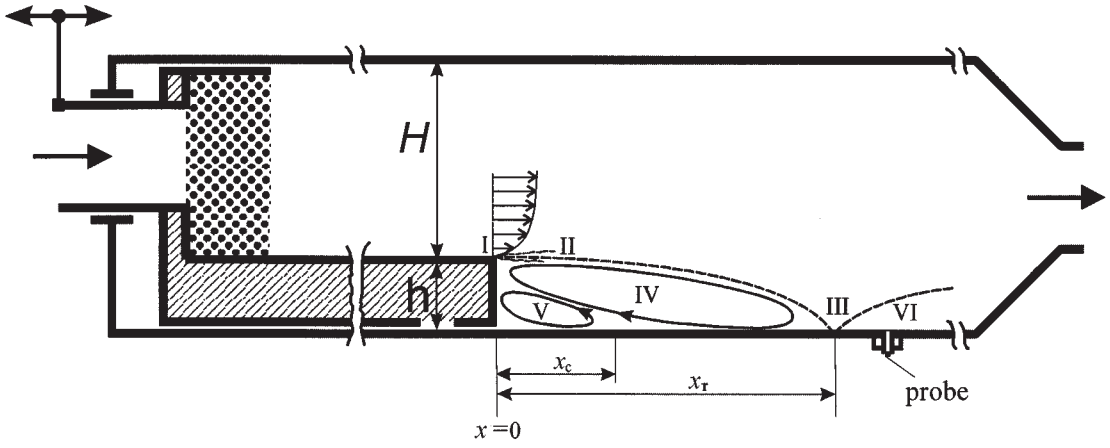

Fig. 2. The backward-facing step apparatus. The flow scheme: Initial boundary layer (I), separated free layer (II), reattachment zone (III), recirculation region (IV) extended to the reattachment point x_r, corner eddy (V) limited by the second separation point x_c, and redeveloping boundary layer (VI).

which was inserted into the channel, formed the step of $h = 20$ mm and caused the channel sudden expansion from the height of $H = 50$ mm (upstream section) to $H+h = 70$ mm (downstream section) giving an expansion ratio, ER = 1.4. The value of channel aspect ratio (channel width/step height) AR = 11 was sufficient to ensure practically two-dimensional flow conditions in the experimental channel. A movable part of the apparatus consisted of an inlet tube, a calming section, and the step block joined together. The three-segment electrodiffusion probe was fixed at the spanwise centreline of the channel and flush mounted in its bottom wall. Due to the upstream section movement, the distance between the step and the probe could be gradually changed in the range of x/h from 0 to 25. A centrifugal pump was used to supply the test fluid from a storage tank (80 dm^3) through a flowmeter into the channel. The measurements covered an initial part of the turbulent flow regime. The Reynolds number was calculated for flow conditions in the upstream section ($Re = UH/\nu$) and ranged from 1200 to 12000.

The test fluid was water containing equimolar 0.025 M potassium ferro/ferricyanide and 0.05 M potassium sulfate as a suitable electrochemical system. The polarization potential of −0.8 V was applied to assure that such an electrolytic cell was working within the range of the limiting current plateau of ferricyanide ions reduction. The three-segment probe of a circular shape was made of three platinum wires deformed by pulling together through a goldsmith-wiredrawing die. These wires were insulated with a deposit of a polymeric paint and, after soldering leads, glued together with an epoxy resin into a stainless steel tube acting as an auxiliary electrode. The front photograph of such a probe is presented in Fig. 3 where the whole active surface of the probe (0.5 mm in diameter) composed of three individual segments can be seen. The probe segments are separated by insulating gaps about 10 mm in the width.

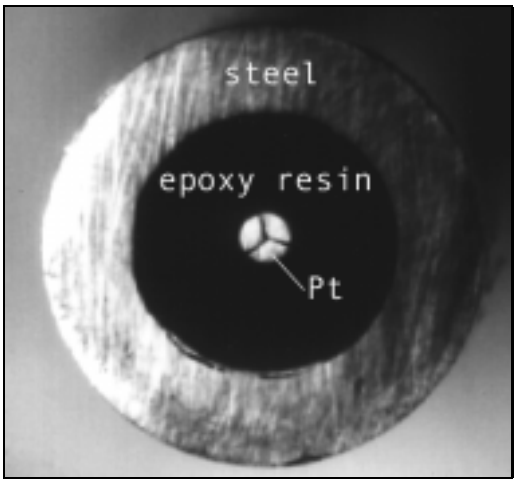

Fig. 3. The three-segment probe (magnified front view).

The probe was calibrated in a special device involving two coaxial cylinders. The probe was inserted into the wall of the outer cylinder and steady flow conditions were provided by rotation of the inner cylinder. It was possible to turn the probe and so to adjust the flow direction angle with respect to the probe axis. The directional characteristics obtained for this probe are shown in Fig. 1. The almost linear parts of these characteristics (six sectors in the middle range of I_s/I) were used for the calculation of instantaneous flow directions during measurements in the channel.

The Drag-Reducing Channel Flow

These experiments were conducted in a rectangular channel made of plexiglass (12 mm in height, 120 mm in width, and 2.6 m in length). To minimize the mechanical polymer degradation the fluid was forced to flow between two tanks (180 dm^3) by imposing an overpressure. Flow rates achieved in the channel corresponded to the Reynolds numbers ranged from 10000 to 35000. The pressure taps were used to measure the pressure drop along the channel.

Experiments were performed with aqueous solutions ($w = 20$—100 ppm) of two high-molecular mass polymers ($M_r \approx 5 \times 10^6$), polyethylene oxide (PEO) and polyacrylamide (PAA). The electrochemical system applied was the same as in the backstep experiments, but the concentrations of active ions were lower (0.003 M ferro/ferricyanide and 0.03 M potassium sulfate). The measurement section with the electrodiffusion electrodes was located 2 m downstream the tank where well-developed turbulent flow conditions were ensured.

Eight double microelectrodes prepared by the photolithography technique were aligned in the direction transversal to the mean flow. Each gold microelectrode (100 μm in the diameter) was divided by an insulating gap (15 μm in the thickness) into two semicircular segments. As can be seen in Fig. 4, the centre-to-centre distance of the two closest microelectrodes was 120 μm. All microelectrodes were simultaneously

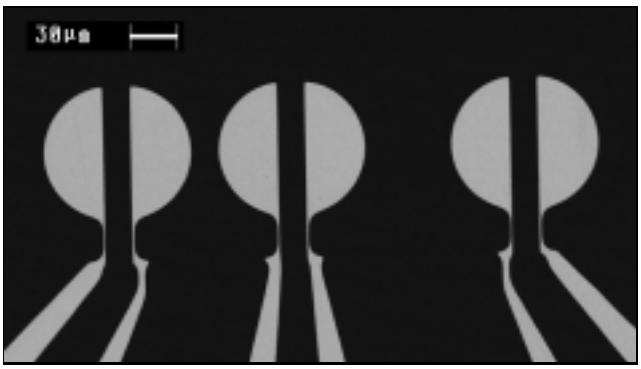

Fig. 4. The double semi-circular probes prepared by the photolithography.

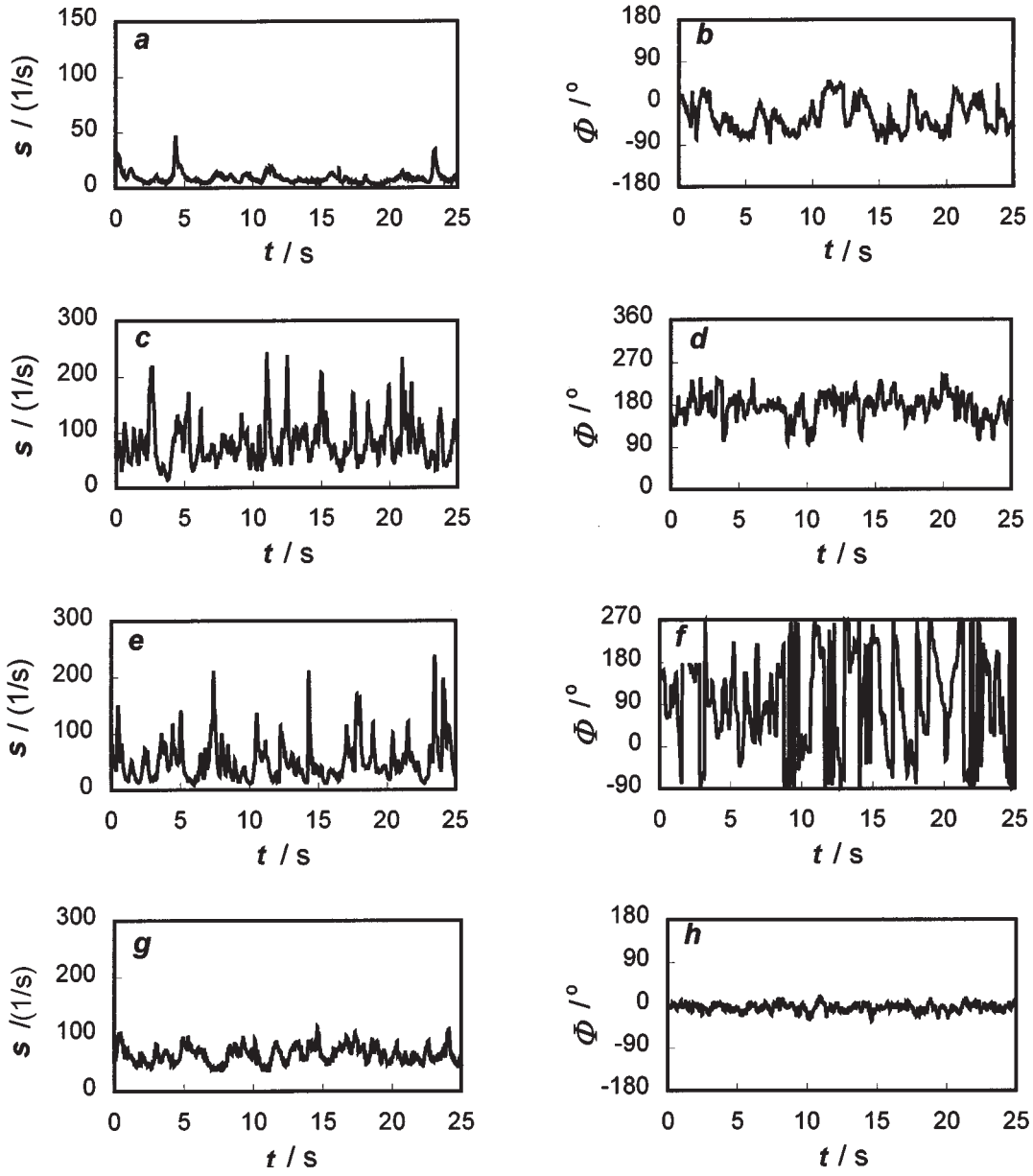

Fig. 5. Time traces of the wall shear rate $s(t)$ and the flow direction angle $\Phi(t)$ ($U = 0.177$ m s^{-1}; $Re = 8840$; $x/h = 1$ (a, b), 3.5 (c, d), 5 (e, f), and 20 (g, h)).

working in the regime of the limiting diffusion current. The current signals from the individual segments provided information on two components of the wall shear rate, axial $s_x \approx I_1 + I_2$ and transverse $s_z \approx I_1 - I_2$. These current signals were amplified, converted to the voltages, and recorded by a TEAC RD-145T data recorder on a tape. The frequency band of these analogue signals was up to 2.5 kHz for each from 16 channels of the recorder.

RESULTS AND DISCUSSION

The Near-Wall Flow Structure behind a Backward-Facing Step

The time traces of the wall shear rate typical for four different flow regions behind the step are shown in Fig. 5. The first couple of traces (Fig. 5*a, b*) reveals a weak secondary recirculation inside the corner eddy situated immediately behind the step, which is marked as the region V in Fig. 2. Small values of the wall shear rate characterize a directionally unsteady flow close to the wall. However, the downstream flow direction predominates in this region ($|\Phi| < 90°$). The second couple of traces (Fig. 5*c, d*) demonstrates the situation inside the primary recirculation region (denoted as the region IV in Fig. 2), where the reverse flow ($\Phi \approx 180°$) appears and the near-wall flow fluctuations are very strong. The third couple of traces (Fig. 5*e, f*) represents the situation close to the reattachment point x_r, where the flow switches periodically between the upstream and downstream directions. Due to a lim-

ited dynamic response of the electrodiffusion probe, the wall shear rate measurement is difficult in this highly unsteady flow region. The probe is not able to follow sudden changes in the flow direction, especially in the case of flow reversal. However, an intermittent character of the flow, with the reverse flow fraction approximately equal to the downstream flow fraction ($90° < \Phi < 270°$ for 48 % of time), can be seen in Fig. 5*f*. As a result, the streamwise wall shear rate component reaches time-average values close to zero near reattachment ($\bar{s}_x = 2.2\ \mathrm{s}^{-1}$ for data presented in Fig. 5*e, f*). The last couple of traces (Fig. 5*g, h*) shows the redeveloping flow far away from reattachment. The downstream flow direction ($\Phi \approx 0°$) is restored again close to the wall, but the low-frequency fluctuations still persist at this long distance from reattachment. These fluctuations, as a residue of large vortices from the free shear layer, slow down the development of the reattached shear layer to an equilibrium state.

The measured probe signals were also converted to the wall shear stress. The time-averaged and fluctuating component of wall shear stress are shown in Fig. 6. The flow regions related to these wall shear stress distributions are obvious from the flow direction mapping also shown in Fig. 6. Small positive values of τ_w close to the step indicate the weak corner eddy. In contrast, negative values of τ_w inside the recirculation region are relatively large. For low flow rates the absolute value of the local minimum reaches the same level as the steady downstream value. This pronounced minimum can be found in the middle of the reverse flow region. Small values of the fluctuating component of wall shear stress τ'_w can be found in the corner region. However, the wall shear stress fluctuations are very large near the reattachment point, where large and energetic eddies are impinging on the wall. The maximum magnitude of near-wall flow fluctuations is achieved approximately one step-height upstream of the reattachment point where the fluctuating component τ'_w reaches about 75 % of the maximum level of τ_w. The streamwise distribution of τ'_w has a similar shape as those very often inferred for wall transfer coefficients [9, 10]. Therefore transfer processes at the wall seem to be controlled by the fluctuating component of wall shear rate in turbulent backstep flows. A more detailed analysis of all results obtained can be found in [11].

The Modification of Near-Wall Turbulence by a High Polymer Addition

The drag reduction percentage, based on pressure drop data measured in the flow channel, $\mathrm{DR} = 100(\Delta P_{\mathrm{water}} - \Delta P_{\mathrm{polymer}})/\Delta P_{\mathrm{water}}$, reached the values up to 75 %. This drag reduction level was affected not only by the polymer concentration, but also by its gradual degradation on a charge of high shear stresses in the channel. The friction data calculated from the electrodiffusion measurements of the wall shear stress ($c_f = 2\tau_w/(\rho u^2)$) and from the pressure drop measurements ($c_f = (h/L)\Delta P/(\rho u^2)$) were compared. A satisfactory agreement between these two types of measurements is demonstrated in Fig. 7.

The power spectrum density (PSD) functions, corresponding to the wall shear rate fluctuations in the axial (W_{SxSx}) and transverse (W_{SzSz}) directions, were calculated from the measured current signals. These spectra were converted from the PSD of the current

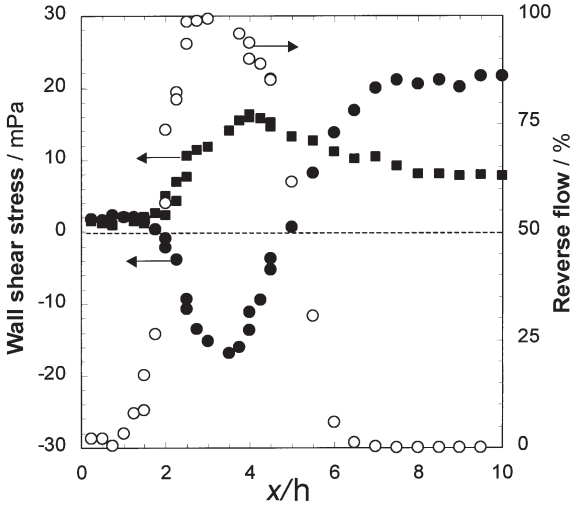

Fig. 6. The streamwise distributions of the wall shear stress measured at $Re = 3860$. The time-averaged (■) and fluctuating (●) components of the wall shear are presented together with the fraction of time during which the near-wall flow is in reverse direction (○).

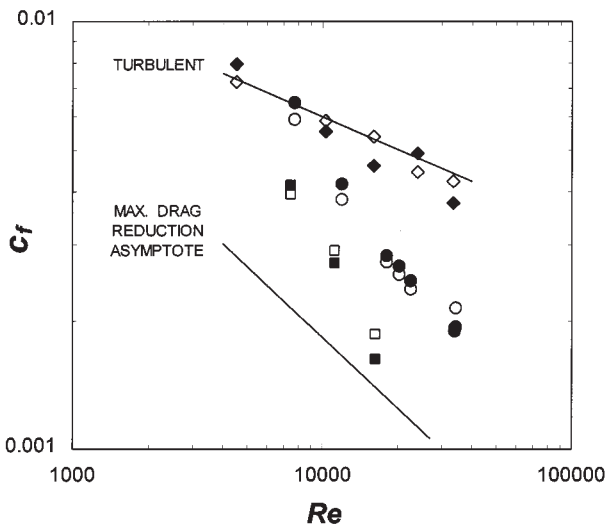

Fig. 7. Comparison of the electrodiffusion (solid symbols) and the pressure drop (open symbols) measurements of the skin friction for experiments carried out with water (diamonds), and with aqueous solutions of 20 ppm PAA (circles), or 50 ppm PEO (squares).

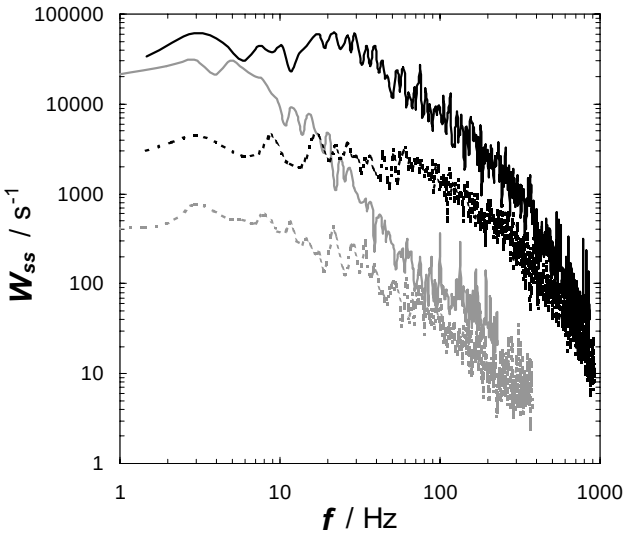

Fig. 8. Effect of drag reduction on the PSD functions of the axial (solid lines) and transverse (dashed lines) components of the wall shear rate fluctuations (black spectra: water, $Re = 18500$; grey spectra: aqueous solution of 50 ppm PAA, $Re = 18100$, DR = 50 %).

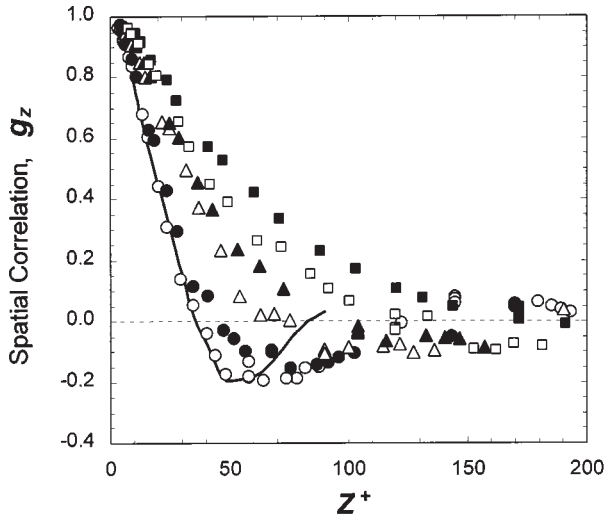

Fig. 9. Lateral correlations of the axial component of wall shear rate calculated from data obtained for water (solid line) and the aqueous solution of 50 ppm PAA at different values of $Re = 6160$ (○), 8620 (●), 12730 (△), 18070 (▲), 21350 (□), and 36550 (■).

fluctuations of $\{I_1 + I_2\}(t)$ and $\{I_1 - I_2\}(t)$ by using the appropriate transfer functions $H(\mathrm{i}2\pi f)$. These frequency-dependent functions relate the power of wall shear rate fluctuations to the power of limiting diffusion current fluctuations

$$W_{SS} = \|H(\mathrm{i}2\pi f)\|^2 W_{\mathrm{II}} \qquad (4)$$

The expressions of H calculated for sinusoidal fluctuations in both the longitudinal and transverse direction can be found in [4, 5].

The effect of drag-reducing polymer on the power spectra of wall shear rate fluctuations is illustrated in Fig. 8. A substantial decrease in PDS function and its frequency redistribution was observed for the polymer solutions with respect to water. As can be also seen in Fig. 8, the flow fluctuations reduction due to the polymer addition is more pronounced in the transverse direction. The turbulent intensities in the axial and transverse directions were determined from the power spectra. The mean values found for water $s'_x/\bar{s}_x = 0.35$ and $s'_z/\bar{s}_x = 0.11$ were in good agreement with the earlier published data [12, 13].

The spatial correlations were calculated from the current signals taken from the double microelectrodes, which were located at eight different transverse positions. The lateral correlation functions g_z obtained for water and the polymer solutions are shown in Fig. 9. An increase in the width of the longitudinally oriented eddies with drag reduction level is striking. The average length scale λ^+, normalized with respect to the wall parameters, was determined from the course of the lateral correlation functions. This length scale, which characterizes the pair of contra-rotating vortices, was calculated as a double of the lateral distance corresponding to the maximum negative correlation. In agreement with the previous experiments [14], practically constant value of $\lambda^+ \approx 100$ was obtained for the turbulent flow of water. For the polymer solutions, this value increased with the level of drag reduction and achieved the value of $\lambda^+ \approx 350$ in the case of DR $\approx$ 75 %.

CONCLUSION

The electrodiffusion technique proved to be applicable to study near-wall flow situations even under highly unsteady, turbulent flow conditions. The multisegment probes provided some valuable information on the near-wall flow structure in two types of the channel flows.

The three-segment probe confirmed the existence of two recirculation zones in the flow behind the backward-facing step. The time-average value of the reattachment length was practically constant after reaching turbulent flow conditions ($x_\mathrm{r}/h \approx 5.1$). The weak corner eddy extended from the step up to the position of second separation ($x_\mathrm{c}/h \approx 1.75$). The intensity of velocity fluctuations parallel to the wall in the near-wall region was found to be of the order of magnitude of local mean velocity. The fluctuating (r.m.s.) component of the wall shear rate seems to control the transfer processes at the wall and also scales the spectral distribution of energy of the near-wall fluctuations in the recirculation zone.

The application of microelectrodes prepared by the photolithography technique gave us a new insight into the turbulence structure in the drag reducing flows. The flow fluctuations close to the wall were greatly re-

duced by addition of polymer and the corresponding power spectra exhibited a shift towards low frequencies. This fluctuation damping was more pronounced for the transverse velocity component. The size of the coherent flow structures was significantly increased due to the drag-reducing additive in both longitudinal and transverse directions.

Acknowledgements. This work was supported by the Ministry of Education, Youth, and Sports of the Czech Republic under the project COST F2.10.

REFERENCES

1. Hanratty, T. J. and Campbell, J. A., *Measurement of wall shear stress*, in *Fluid Mechanics Measurement.* (Goldstein, J. R., Editor.) P. 559. Hemisphere, Washington, 1983.
2. Wein, O. and Sobolík, V., *Collect. Czech. Chem. Commun. 52*, 2169 (1987).
3. Sobolík, V., Wein, O., Gil, O., and Tribollet, B., *Exp. Fluids 9*, 43 (1990).
4. Deslouis, C., Huet, F., Gil, O., and Tribollet, B., *Exp. Fluids 16*, 97 (1993).
5. Deslouis, C., Gil, O., and Tribollet, B., *J. Fluid Mech. 215*, 85 (1990).
6. Hanratty, T. J. and Mao, Z., *Int. J. Heat Mass Transfer 34*, 281 (1991).
7. Tihon, J. and Sobolík, V., *Proc. 3rd Int. Workshop "ED Diagnostics of Flow".* (Deslouis, C. and Tribollet, B., Editors.) P. 397. Dourdan, 1993.
8. Wein, O., Sobolík, V., and Tihon, J., *Collect. Czech. Chem. Commun. 62*, 420 (1997).
9. Tagg, D. J., Patrick, M. A., and Wragg, A. A., *Trans. Inst. Chem. Eng. 57*, 176 (1979).
10. Vogel, J. C. and Eaton, J. K., *J. Heat Transfer 107*, 922 (1985).
11. Tihon, J., Legrand, J., and Legentihomme, P., *Exp. Fluids 31,* 484 (2001).
12. Hanratty, T. J., Chorn, L. G., and Hatziavramidis, D. T., *Phys. Fluids 10*, 112 (1977).
13. Phillips, W. R. C., *Phys. Fluids 30*, 2354 (1987).
14. Kline, S. J., Reynolds, W. C., Schraub, F. A., and Runstadler, P. W., *J. Fluid Mech. 30,* 741 (1967).